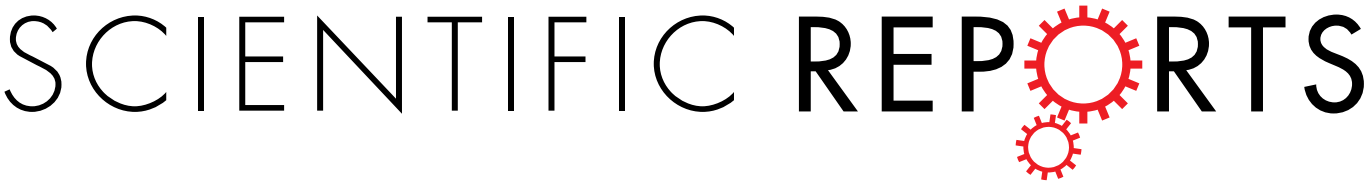

OPEN

Precisely Determining Ultralow level UO_2^{2+} in Natural Water with Plasmonic Nanowire Interstice Sensor

Received: 30 September 2015
Accepted: 15 December 2015
Published: 21 January 2016

Raekeun Gwak[1,*], Hongki Kim[1,*], Seung Min Yoo[2], Sang Yup Lee[2], Gyoung-Ja Lee[3], Min-Ku Lee[3], Chang-Kyu Rhee[3], Taejoon Kang[4,5] & Bongsoo Kim[1]

Uranium is an essential raw material in nuclear energy generation; however, its use raises concerns about the possibility of severe damage to human health and the natural environment. In this work, we report an ultrasensitive uranyl ion (UO_2^{2+}) detection method in natural water that uses a plasmonic nanowire interstice (PNI) sensor combined with a DNAzyme-cleaved reaction. UO_2^{2+} induces the cleavage of DNAzymes into enzyme strands and released strands, which include Raman-active molecules. A PNI sensor can capture the released strands, providing strong surface-enhanced Raman scattering signal. The combination of a PNI sensor and a DNAzyme-cleaved reaction significantly improves the UO_2^{2+} detection performance, resulting in a detection limit of 1 pM and high selectivity. More importantly, the PNI sensor operates perfectly, even in UO_2^{2+}-contaminated natural water samples. This suggests the potential usefulness of a PNI sensor in practical UO_2^{2+}-sensing applications. We anticipate that diverse toxic metal ions can be detected by applying various ion-specific DNA-based ligands to PNI sensors.

Uranium, a representative radioactive metal, has been used as the main source of nuclear power generation via nuclear fission[1]. Uranium can exist in various forms in the environment, such as uranyl fluoride (UO_2F_2), uranyl tetrafluoride (UF_4), uranium dioxide (UO_2), and triuranium octoxide (U_3O_8). The accumulation of these compounds in the human body can lead to severe health problems[2]. For example, UO_2F_2 and UF_4 cause kidney damage, and UO_2 and U_3O_8 can cause certain cancers and mutations by accumulating in the lungs[3]. Uranium is also found in diverse forms in aqueous conditions. The uranyl ion (UO_2^{2+}) is the most soluble and common form[4,5]. Because UO_2^{2+} can disturb organ function by accumulating in the skeleton, kidneys, lungs, and liver[6,7], the detection of UO_2^{2+} in natural water is very important.

Traditionally, UO_2^{2+} has been detected using various physical and chemical techniques, including inductively coupled plasma-mass spectrometry[8], radio spectrometry[9], atomic adsorption spectrometry[10], and phosphorimetry[11]. However, these methods present several drawbacks in that they require expensive instruments, involve complicated methods, and are time-consuming. Recently, nanomaterial-based UO_2^{2+} sensing methods have been developed by employing fluorescence[12,13], electrochemistry[14], resonance scattering[15,16], colorimetry[17], magnetoelasticity[18], and surface-enhanced Raman scattering (SERS)[19–21]. Among these techniques, SERS offers highly sensitive molecular detection because SERS signals can be obtained from a small number of molecules or even a single molecule located within a sub-10 nm metallic nano-gap (hot spot)[22–42]. This technique also provides molecular fingerprints and causes less photobleaching[43–48]. Nevertheless, there are only a few reported SERS sensors for UO_2^{2+} detection, and most of them have not been validated in real environments. Therefore, further improvements in sensitivity, selectivity, and reproducibility are still needed for the practical sensing of UO_2^{2+} in a real environment using a SERS sensor.

[1]KAIST, Department of Chemistry, Daejeon 34141, Korea. [2]KAIST, Department of Chemical and Biomolecular Engineering, Daejeon 34141, Korea. [3]KAERI, Nuclear Materials Development Division, Daejeon 34057, Korea. [4]KRIBB, BioNanotechnology Research Center and BioNano Health Guard Research Center, Daejeon 34141, Korea. [5]UST, Major of Nanobiotechnology and Bioinformatics, Daejeon 34113, Korea. *These authors contributed equally to this work. Correspondence and requests for materials should be addressed to T.K. (email: kangtaejoon@kribb.re.kr) or B.K. (email: bongsoo@kaist.ac.kr)

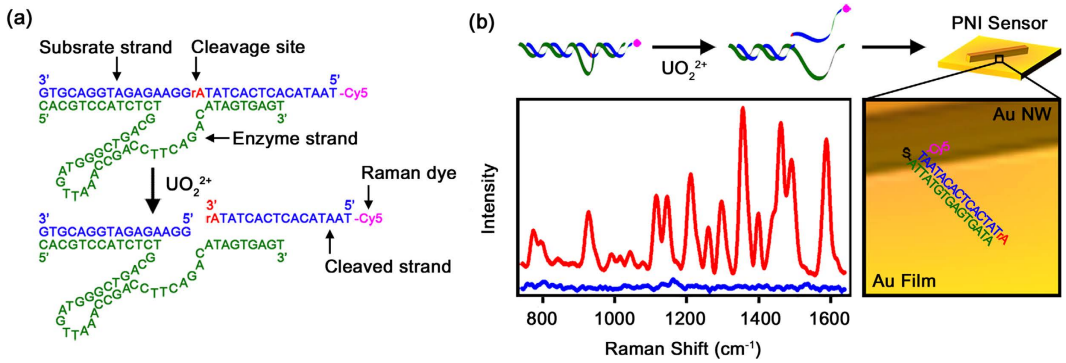

Figure 1. (**a**) Schematic illustration of UO_2^{2+}-specific DNAzyme and cleavage of DNAzyme induced by UO_2^{2+} (**b**) Schematic illustration of UO_2^{2+} detection by a PNI sensor combined with a DNAzyme-cleaved reaction. The left panel shows the SERS spectra measured from PNI sensors in the absence of (blue spectrum) and the presence of 10 nM UO_2^{2+} (red spectrum).

Here, we report an ultrasensitive UO_2^{2+} detection method using a plasmonic nanowire (NW) interstice (PNI) sensor combined with a DNAzyme-cleaved reaction. SERS-based sensing methods are often affected by uncontrolled aggregation and size distribution of nanomaterials, which are detrimental to the reproducibility of the sensor[49–51]. A PNI platform composed of a single-crystalline Au NW with an atomically flat surface has shown improved sensitivity and reproducibility[31]. By combining the DNAzyme cleaving method with a PNI platform, we quantitatively detected UO_2^{2+} with an ultralow detection limit of 1 pM and high selectivity. More importantly, the precise detection of UO_2^{2+} was demonstrated in several UO_2^{2+}-contaminated natural water samples, showing the practical applicability of the PNI sensor.

Results and Discussion

DNA-based ligands, including aptamers and DNAzymes, have been widely used to detect various metal ions because they provide several advantages, such as high affinity, selectivity, stability, and relative ease of modification[52,53]. In this experiment, we used a DNAzyme, which has the sequence shown in Fig. 1a, for the detection of UO_2^{2+}. A DNAzyme is composed of an enzyme strand and a substrate strand. The enzyme strand (green) is a specific sequence that can bind to UO_2^{2+}. The substrate strand (blue) is hybridized with the enzyme strand. In the middle of the substrate strand, a ribose-adenosine (rA) sequence (red) is present. Ribonucleotides are approximately 100,000-fold more susceptible to hydrolytic cleavage than deoxyribonucleotides[13]. At the 5′ end of the substrate strand, Cy5 (magenta) is present. Cy5 is a well-known Raman reporter for the 633 nm excitation source[27–32]. When UO_2^{2+} was added to DNAzyme, UO_2^{2+} bound to the enzyme strand, and thus, the rA sequence on the substrate strand was hydrolytically cleaved. The cleaved strand was released from the DNAzyme and then captured by a PNI sensor. The PNI sensor was prepared by laying down a single-crystalline Au NW onto a Au film[24] (Fig. 1b). Au NWs were synthesized using a previously reported vapor transport method[54] and then modified by the addition of a complementary capture DNA strand to the cleaved strand. The length of capture strand was set as 15 base pairs to increase the hybridization efficiency with cleaved strand[55]. The PNI sensor with an attached cleaved strand can provide a strong Cy5 SERS signal, enabling the detection of UO_2^{2+}. The left panel in Fig. 1b shows the result of using a PNI sensor combined with a DNAzyme-cleaved reaction for UO_2^{2+} detection. When UO_2^{2+} was present in the sample solution at the concentration of 10 nM, 4 major bands at 1185, 1360, 1485, and 1580 cm^{-1} were clearly detected by the PNI sensor (red spectrum). These bands correspond to the $\nu(C\text{-}N)_{stretch}$, $\nu(C=C)_{ring}$, $\nu(C\text{-}C)_{ring}$, and $\nu(C=N)_{stretch}$ of Cy5, respectively[28]. In contrast, when UO_2^{2+} was absent from the sample solution, the PNI sensor exhibited a weak SERS signal (blue spectrum). In this way, UO_2^{2+} can be detected from the turn-on of the SERS signal. Generally, turn-on type sensors are more suitable than turn-off type sensors for practical applications because they result in fewer false-positive results[17].

Figure 2a shows the SERS signals measured from the PNI sensors while varying the UO_2^{2+} concentration from 1 pM to 100 nM. The samples were prepared by a 1/10 serial dilution, and a blank sample solution was prepared as a control. In the blank sample solution, the PNI sensor provided a weak Cy5 SERS signal (black spectrum in Fig. 2a). In the 1 pM sample, the signal was significantly enhanced (red spectrum in Fig. 2a). Figure 2b shows the intensity of the Cy5 1580 cm^{-1} band plotted as a function of the UO_2^{2+} concentration. The SERS signal from the PNI sensor increased as the UO_2^{2+} concentration increased, saturating at a concentration of 10 nM. The inset in Fig. 2b shows the dynamic range of the PNI sensor for UO_2^{2+} detection. The SERS signal intensity linearly increased within the UO_2^{2+} concentration range of 1 pM to 10 nM. This wide dynamic range makes this technique advantageous for the quantitative detection of UO_2^{2+}. We estimated the detection limit of the PNI sensor to be 1 pM. This detection limit is approximately 1,000-fold lower than the limits of other SERS-based sensors[21]. Furthermore, the detection limit of this method is comparable to that of the most sensitive detection method, which is based on a resonance scattering spectral technique[15].

To confirm the selectivity of a PNI sensor combined with a DNAzyme-cleaved reaction, SERS signals were observed from the PNI sensors after mixing DNAzyme with samples containing various metal ions (UO_2^{2+}, Cd^{2+}, Hg^{2+}, Pb^{2+}, Ca^{2+}, Mg^{2+}, Zn^{2+}, Cu^{2+}, Fe^{2+}, Co^{2+}, Ni^{2+}, and Th^{4+}). The concentration of each metal ion was 10 nM. Figure 3 shows the intensity of the Cy5 1580 cm^{-1} band measured from the PNI sensors for detecting the various

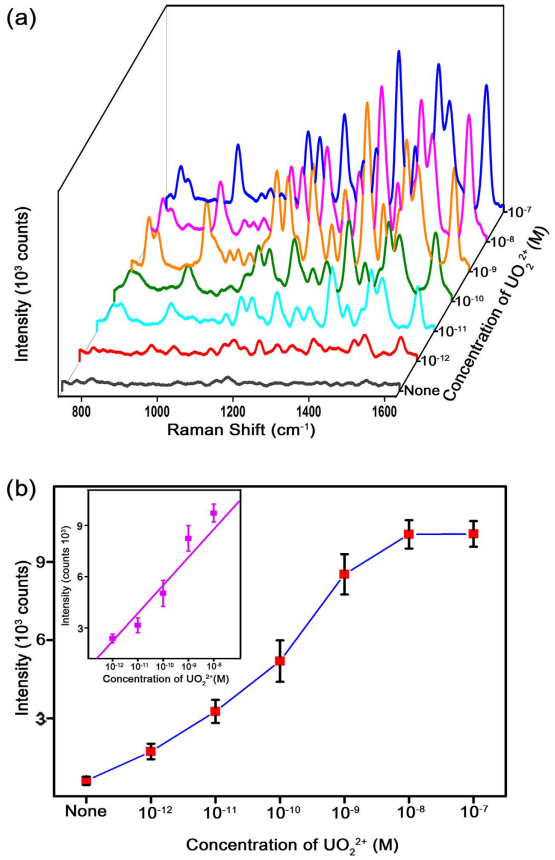

Figure 2. (**a**) SERS spectra of Cy5 measured from PNI sensors when the UO_2^{2+} concentration is varied from 1 pM to 100 nM. (**b**) Intensity of the Cy5 1580 cm^{-1} band plotted as a function of the UO_2^{2+} concentration. The inset provides the dynamic range of the PNI sensor for UO_2^{2+} detection. The data represent the mean plus standard deviation from 7 measurements.

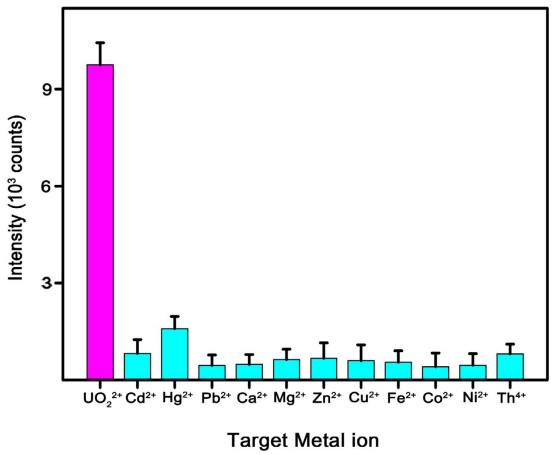

Figure 3. Selectivity of a PNI sensor for UO_2^{2+} detection. The tested metal ions are shown on the *x* axis and their corresponding Cy5 1580 cm^{-1} band intensities are shown on the *y* axis. Strong SERS signals were observed only in the presence of UO_2^{2+} (magenta bar) and weak SERS signals were observed in the presence of other metal ions (cyan bars). The data represent the mean plus standard deviation from 7 measurements.

metal ions. Remarkable SERS signal was observed only in the presence of UO_2^{2+} (magenta bar in Fig. 3), and no distinct SERS signal was observed in the presence of other metal ions (cyan bars in Fig. 3). These results indicate that the proposed detection method is highly specific for UO_2^{2+}.

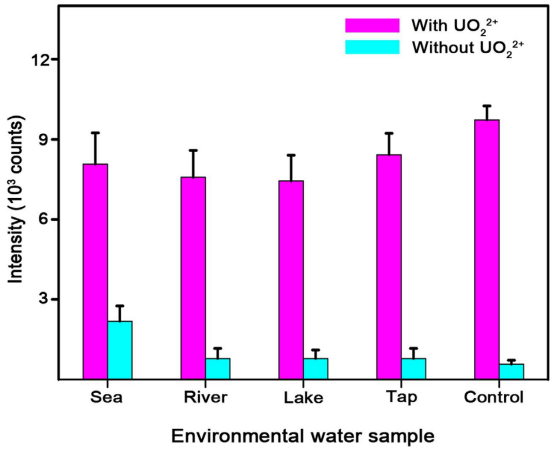

Figure 4. Applicability of a PNI sensor for UO_2^{2+} detection in natural water. Natural water samples are shown on the *x* axis and their corresponding Cy5 1580 cm^{-1} band intensities are shown on the *y* axis. The magenta bars represent the natural water samples spiked with UO_2^{2+} and the cyan bars represent the as-collected natural water samples. The spiked UO_2^{2+} concentration was 10 nM. The strong SERS signals were observed only after the addition of UO_2^{2+} into the natural water samples. The data represent the mean plus standard deviation from 7 measurements.

Finally, we examined the applicability of a PNI sensor combined with a DNAzyme-cleaved reaction to detect UO_2^{2+} in natural water. The natural water samples were obtained from various environments, including a sea, a river, a lake, and a tap. Buffer solution was also prepared as a control. Figure 4 shows the intensities of the Cy5 1580 cm^{-1} band measured from the PNI sensors after mixing DNAzyme with the natural water samples. The magenta bars represent the natural water samples spiked with UO_2^{2+} and the cyan bars represent the as-collected natural water samples. Strong SERS signals were observed only after the addition of UO_2^{2+} into the natural water samples. Without UO_2^{2+}, SERS signals were rarely observed. Note that the DNAzyme is sensitive to ionic strength[56]. The DNAzyme is in the lock-and key mode at the ionic strength of 100 mM or higher[56]. In addition, the concentration of Mg^{2+} can affect the DNAzyme activity[56]. At the lower concentration of 2 mM, the activity is promoted. On the other hand, the activity is inhibited at the higher concentration of 2 mM. In this experiment, the DNAzyme solution and natural water sample were mixed with 9:1 volume ratio before the SERS measurement. The ionic strengths of the mixtures are calculated as 246.43 mM (sea), 131.81 mM (river), 134.72 mM (lake), and 132.07 mM (tap) according to the inductively coupled plasma-optical emission spectroscopy (ICP-OES) and ion chromatography (IC) data of natural water samples (Table S1 and S2 in supplementary information). The concentrations of Mg^{2+} in the mixtures are 1.31 mM (sea), 0.01 mM (river), 0.02 mM (lake), and 0.01 mM (tap). Since the ionic strengths of mixtures are higher than 100 mM and the concentrations of Mg^{2+} in the mixtures are below 2 mM, the PNI sensor combined with a DNAzyme-cleaved reaction can detect UO_2^{2+} successfully even in natural water samples. The USA's limit for UO_2^{2+} in drinking water is 30 μg/L (approximately 100 nM), however, the long-term consumption and exposure to water that contains UO_2^{2+}, even at concentrations below this limit, can cause severe toxicity and serious diseases[57]. We anticipate that the present method can be employed for practical UO_2^{2+} detection and aid in the prevention of environmental pollution and human diseases caused by UO_2^{2+}.

Conclusion

We detected UO_2^{2+} by combining an ultrasensitive PNI platform with a DNAzyme-cleaved reaction. The DNAzyme specifically reacted with UO_2^{2+} and released a cleaved strand. The PNI sensor sensitively captured the cleaved strand, which enabled the detection of UO_2^{2+}. We quantitatively detected UO_2^{2+} with an ultralow detection limit of 1 pM and high selectivity. Moreover, this method enables the detection of UO_2^{2+} in various natural water sources, such as sea, lake, river, and tap. A PNI sensor that can precisely detect small quantities of UO_2^{2+} in natural water is expected to reveal many environmental pollutants, and hence minimize damage to the human body caused by UO_2^{2+} exposure.

Methods

Materials. Purified DNA was purchased from Bioneer (Daejeon, Korea). $Hg(Ac)_2$, $Mg(Ac)_2$, $Ca(Ac)_2$, $CrCl_2$, $FeCl_2$, $Co(Ac)_2$, $NiCl_2$, $CuCl_2$, $Zn(Ac)_2$, $Cd(Ac)_2$, $Pb(Ac)_2$, $UO_2(Ac)_2$, Au powder (99.99%), and sodium dodecyl sulfate (SDS) were purchased from Sigma–Aldrich. $Th(NO_3)_4$ was purchased from Merck. Phosphate buffered saline (PBS) was purchased from Gibco. The natural water samples were collected from the west sea of South Korea, the Gap River, and the pond at KAIST. Samples were centrifuged to remove impurities.

Preparation of DNAzyme. The sequence of the substrate strand is 5′-Cy5-TAATACACTCACTAT(rA)GGAAGAGATGGACGTG-3′, and the sequence of the enzyme strand is 5′-CACGTCCATCTCTGCAGTCGGGTAGTTAAACCGACCTTCAGACATAGTGAGT-3′. The sequence of the capture strand is 5′-ATAGTGAGTGTATTA-SH-3′. The substrate and enzyme strands were mixed in a 1× PBS solution (pH 7.4) at the

same molar concentration (10 μM each). The hybrid solutions were heated at 95 °C for 10 min and slowly cooled to room temperature.

Synthesis of single-crystalline Au NWs. Single-crystalline Au NWs were synthesized on a *c*-cut sapphire substrate in a horizontal quartz tube furnace system following the chemical vapor transport method described in a previous report[54]. An alumina boat containing an Au powder was positioned directly below the heat source. The sapphire substrate was placed a few centimeters downstream from the alumina boat. The heating zone was brought to 1100 °C while the chamber pressure was maintained at 3–5 Torr. Ar gas flowing at 100 sccm was used to transport the Au vapor. Au NWs were grown on the sapphire substrate over a 1 h period.

Preparation of PNI sensors. Au film substrates were prepared on Si substrates by electron beam-assisted deposition of a 10 nm thick film of Cr followed by a 300 nm thick film of Au. The prepared Au films were SERS-inactive by themselves[24]. The Au films were then cut to 1 cm^2 for PNI sensor fabrication. To prepare the capture probe DNA-attached Au NWs, as-synthesized NWs were incubated with 5 mM captured DNA in 1 M KH_2PO_4 buffer (pH 6.75) at room temperature for 12 h. Next, the Au NWs were rinsed with a 0.2% (w/v) SDS solution for 5 min. The capture probe DNA-attached Au NWs were then transferred onto Au films by a simple attachment and detachment process[30]. Briefly, the NW-grown *c*-cut sapphire substrates were inverted onto Au film substrates containing medium. Before both substrates were overlapped, a drop of distilled water was applied as a lubricant. The sapphire substrates were then pushed gently and, after a few seconds, detached. After the attachment and detachment process, the remaining water was dried under flowing N_2 gas.

Detection of UO_2^{2+} using PNI sensors combined with a DNAzyme-cleaved reaction. DNAzyme in 1× PBS (pH 7.4) with RNase-free water was mixed with sample solutions containing 0.27% (w/v) HNO_3 and incubated for 10 min. The pH of the mixed solution was maintained at 5.49 and its ionic strength was 146.43 mM. To stop the enzymatic reaction by shifting the pH of the mixture, 0.1 mM Tris-acetate solution was added. Then, the mixture was dropped onto the PNI sensor and allowed to stand for 2 h. To remove excess DNA, the sensor was rinsed with a 0.2% (w/v) SDS solution for 5 min and then rinsed twice with distilled deionized water.

Instrumentation. SERS spectra were measured using a micro-Raman system on an Olympus BX41 microscope. A 633 nm He/Ne laser (Melles Griot) was used as an excitation source, and the laser was focused on samples through a 100× objective (NA = 0.7, Mitutoyo). The laser power directed at the sample was 0.4 mW. The SERS signals were recorded with a thermodynamically cooled electron-multiplying charge-coupled device (Andor) mounted on the spectrometer with a 1200 groove/mm grating. The acquisition time for all SERS spectra was 60 s. A holographic notch filter was used to reject laser light. The concentration of metal ion in natural water samples was analyzed by inductively coupled plasma-optical emission spectroscopy (ICP-OES 720, Agilent) and ion chromatography (881 Compact IC pro, Metrohm Ltd.).

References

1. Cantaluppi, C. & Degetto, S. Civilian and military uses of depleted uranium: environmental and health problems. *ANNALI DI CHIMICA-ROMA-* **90,** 665–676 (2000).
2. Craft, E. S. *et al.* Depleted and natural uranium: chemistry and toxicological effects. *Journal of Toxicology and Environmental Health, Part B* **7,** 297–317 (2004).
3. Chazel, V., Houpert, P. & Ansoborlo, E. Effect of U3O8 specific surface area on *in vitro* dissolution, biokinetics, and dose coefficients. *Radiation protection dosimetry* **79,** 39–42 (1998).
4. Sheppard, S. C. & Evenden, W. G. Bioavailability indices for uranium: effect of concentration in eleven soils. *Archives of Environmental Contamination and Toxicology* **23,** 117–124 (1992).
5. Zhou, P. & Gu, B. Extraction of oxidized and reduced forms of uranium from contaminated soils: Effects of carbonate concentration and pH. *Environmental science & technology* **39,** 4435–4440 (2005).
6. Fisenne, I., Perry, P. & Harley, N. Uranium in humans. *Radiation Protection Dosimetry* **24,** 127–131 (1988).
7. Zamora, M. L., Tracy, B., Zielinski, J., Meyerhof, D. & Moss, M. Chronic ingestion of uranium in drinking water: a study of kidney bioeffects in humans. *Toxicological Sciences* **43,** 68–77 (1998).
8. Boomer, D. & Powell, M. Determination of uranium in environmental samples using inductively coupled plasma mass spectrometry. *Analytical chemistry* **59,** 2810–2813 (1987).
9. Holzbecher, J. & Ryen, D. E. Determination of uranium by thermal and epithermal neutron activation in natural waters and in human urine. *Analytica Chimica Acta* **119,** 405–408 (1980).
10. Mlakar, M. & Branica, M. Stripping voltammetric determination of trace levels of uranium by synergic adsorption. *Analytica chimica acta* **221,** 279–287 (1989).
11. Brina, R. & Miller, A. G. Direct detection of trace levels of uranium by laser-induced kinetic phosphorimetry. *Analytical Chemistry* **64,** 1413–1418 (1992).
12. Wu, P., Hwang, K., Lan, T. & Lu, Y. A DNAzyme-gold nanoparticle probe for uranyl ion in living cells. *Journal of the American Chemical Society* **135,** 5254–5257 (2013).
13. Liu, J. *et al.* A catalytic beacon sensor for uranium with parts-per-trillion sensitivity and millionfold selectivity. *Proceedings of the National Academy of Sciences* **104,** 2056–2061 (2007).
14. Ziółkowski, R., Górski, Ł., Oszwałdowski, S. & Malinowska, E. Electrochemical uranyl biosensor with DNA oligonucleotides as receptor layer. *Analytical and bioanalytical chemistry* **402,** 2259–2266 (2012).
15. Jiang, Z. *et al.* Free-labeled nanogold catalytic detection of trace UO_2^{2+} based on the aptamer reaction and gold particle resonance scattering effect. *Plasmonics* **7,** 185–190 (2012).
16. Zhou, B. *et al.* Resonance light scattering determination of uranyl based on labeled DNAzyme–gold nanoparticle system. *Spectrochimica Acta Part A: Molecular and Biomolecular Spectroscopy* **110,** 419–424 (2013).
17. Lee, J. H., Wang, Z., Liu, J. & Lu, Y. Highly sensitive and selective colorimetric sensors for uranyl (UO_2^{2+}): Development and comparison of labeled and label-free DNAzyme-gold nanoparticle systems. *Journal of the American Chemical Society* **130,** 14217–14226 (2008).
18. Yin, J.-C. *et al.* A wireless magnetoelastic sensor for uranyl using DNAzyme–graphene oxide and gold nanoparticles-based amplification. *Sensors and Actuators B: Chemical* **188,** 147–155 (2013).

19. Bao, L., Mahurin, S., Haire, R. & Dai, S. Silver-doped sol-gel film as a surface-enhanced Raman scattering substrate for detection of uranyl and neptunyl ions. *Analytical chemistry* **75,** 6614–6620 (2003).
20. Dutta, S. *et al.* Silver nanoparticle decorated reduced graphene oxide (rGO) nanosheet: a platform for SERS based low-level detection of uranyl ion. *ACS applied materials & interfaces* **5,** 8724–8732 (2013).
21. Jiang, Z. *et al.* A label-free nanogold DNAzyme-cleaved surface-enhanced resonance Raman scattering method for trace UO_2^{2+} using rhodamine 6G as probe. *Plasmonics* **8,** 803–810 (2013).
22. Kneipp, K. *et al.* Single molecule detection using surface-enhanced Raman scattering (SERS). *Physical review letters* **78,** 1667 (1997).
23. Nie, S. & Emory, S. R. Probing single molecules and single nanoparticles by surface-enhanced Raman scattering. *Science* **275,** 1102–1106 (1997).
24. Yoon, I. *et al.* Single nanowire on a film as an efficient SERS-active platform. *Journal of the American Chemical Society* **131,** 758–762 (2008).
25. Kang, T. *et al.* Creating well-defined hot spots for surface-enhanced Raman scattering by single-crystalline noble metal nanowire pairs. *The Journal of Physical Chemistry C* **113,** 7492–7496 (2009).
26. Kim, J.-H. *et al.* A well-ordered flower-like gold nanostructure for integrated sensors via surface-enhanced Raman scattering. *Nanotechnology* **20,** 235302 (2009).
27. Kang, T., Yoo, S. M., Yoon, I., Lee, S. Y. & Kim, B. Patterned multiplex pathogen DNA detection by Au particle-on-wire SERS sensor. *Nano letters* **10,** 1189–1193 (2010).
28. Kang, T. *et al.* Au Nanowire-on-Film SERRS Sensor for Ultrasensitive Hg^{2+} Detection. *Chemistry-A European Journal* **17,** 2211–2214 (2011).
29. Yoo, S. M. *et al.* Combining a nanowire SERRS sensor and a target recycling reaction for ultrasensitive and multiplex identification of pathogenic fungi. *Small* **7,** 3371–3376 (2011).
30. Kim, H. *et al.* Facile Fabrication of Multi-targeted and Stable Biochemical SERS Sensors. *Chemistry-A Asian Journal* **8,** 3010–3014 (2013).
31. Kang, T. *et al.* Ultra-Specific Zeptomole MicroRNA Detection by Plasmonic Nanowire Interstice Sensor with Bi-Temperature Hybridization. *Small* **10,** 4200–4206 (2014).
32. Kang, T. *et al.* Single-step multiplex detection of toxic metal ions by Au nanowires-on-chip sensor using reporter elimination. *Lab on a Chip* **12,** 3077–3081 (2012).
33. Seol, M.-L. *et al.* A nanoforest structure for practical surface-enhanced Raman scattering substrates. *Nanotechnology* **23,** 095301 (2012).
34. Zhang, Z., Yang, P., Xu, H. & Zheng, H. Surface enhanced fluorescence and Raman scattering by gold nanoparticle dimers and trimers. *Journal of Applied Physics* **113,** 033102 (2013).
35. Seol, M.-L. *et al.* Multi-layer nanogap array for high-performance SERS substrate. *Nanotechnology* **22,** 235303 (2011).
36. Yin, J. *et al.* SERS-active nanoparticles for sensitive and selective detection of cadmium ion (Cd^{2+}). *Chemistry of Materials* **23,** 4756–4764 (2011).
37. Chang, S., Ko, H., Singamaneni, S., Gunawidjaja, R. & Tsukruk, V. V. Nanoporous membranes with mixed nanoclusters for Raman-based label-free monitoring of peroxide compounds. *Analytical chemistry* **81,** 5740–5748 (2009).
38. Gupta, M. K. *et al.* pH-Triggered SERS via Modulated Plasmonic Coupling in Individual Bimetallic Nanocobs. *Small* **7,** 1192–1198 (2011).
39. Chon, H., Lee, S., Son, S. W., Oh, C. H. & Choo, J. Highly sensitive immunoassay of lung cancer marker carcinoembryonic antigen using surface-enhanced Raman scattering of hollow gold nanospheres. *Analytical chemistry* **81,** 3029–3034 (2009).
40. Chung, E., Jeon, J., Yu, J., Lee, C. & Choo, J. Surface-enhanced Raman scattering aptasensor for ultrasensitive trace analysis of bisphenol A. *Biosensors and Bioelectronics* **64,** 560–565 (2015).
41. Lee, J.-H., You, M.-H., Kim, G.-H. & Nam, J.-M. Plasmonic Nanosnowmen with a Conductive Junction as Highly Tunable Nanoantenna Structures and Sensitive, Quantitative and Multiplexable Surface-Enhanced Raman Scattering Probes. *Nano letters* **14,** 6217–6225 (2014).
42. Alexander, K. D. *et al.* A high-throughput method for controlled hot-spot fabrication in SERS-active gold nanoparticle dimer arrays. *Journal of Raman Spectroscopy* **40,** 2171–2175 (2009).
43. Kleinman, S. L., Frontiera, R. R., Henry, A.-I., Dieringer, J. A. & Van Duyne, R. P. Creating, characterizing, and controlling chemistry with SERS hot spots. *Physical Chemistry Chemical Physics* **15,** 21–36 (2013).
44. Haes, A. J., Zou, S., Schatz, G. C. & Van Duyne, R. P. A nanoscale optical biosensor: the long range distance dependence of the localized surface plasmon resonance of noble metal nanoparticles. *The Journal of Physical Chemistry B* **108,** 109–116 (2004).
45. Moskovits, M. Surface-enhanced Raman spectroscopy: a brief retrospective. *Journal of Raman Spectroscopy* **36,** 485–496 (2005).
46. Jain, P. K., Huang, X., El-Sayed, I. H. & El-Sayed, M. A. Review of some interesting surface plasmon resonance-enhanced properties of noble metal nanoparticles and their applications to biosystems. *Plasmonics* **2,** 107–118 (2007).
47. Lee, H., Lee, J.-H., Jin, S. M., Suh, Y. D. & Nam, J.-M. Single-Molecule and Single-Particle-Based Correlation Studies between Localized Surface Plasmons of Dimeric Nanostructures with ~1 nm Gap and Surface-Enhanced Raman Scattering. *Nano letters* **13,** 6113–6121 (2013).
48. Hu, J. *et al.* Sub-attomolar HIV-1 DNA detection using surface-enhanced Raman spectroscopy. *Analyst* **135,** 1084–1089 (2010).
49. Li, W. *et al.* Etching and dimerization: a simple and versatile route to dimers of silver nanospheres with a range of sizes. *Angewandte Chemie International Edition* **49,** 164–168 (2010).
50. Laurence, T. A. *et al.* Rapid, solution-based characterization of optimized SERS nanoparticle substrates. *Journal of the American Chemical Society* **131,** 162–169 (2008).
51. Wei, X. *et al.* A Molecular Beacon-Based Signal-Off Surface-Enhanced Raman Scattering Strategy for Highly Sensitive, Reproducible, and Multiplexed DNA Detection. *Small* **9,** 2493–2499 (2013).
52. Silverman, S. K. *In vitro* selection, characterization, and application of deoxyribozymes that cleave RNA. *Nucleic acids research* **33,** 6151–6163 (2005).
53. Brown, A. K., Liu, J., He, Y. & Lu, Y. Biochemical Characterization of a Uranyl Ion-Specific DNAzyme. *ChemBioChem* **10,** 486–492 (2009).
54. Yoo, Y. *et al.* Steering epitaxial alignment of Au, Pd, and AuPd nanowire arrays by atom flux change. *Nano letters* **10,** 432–438 (2010).
55. Markham, N. R. & Zuker, M. DINAMelt web server for nucleic acid melting prediction. *Nucleic Acids Res.*, **33,** W577–W581 (2005).
56. He, Y. & Lu, Y. Metal-Ion-Dependent Folding of a Uranyl-Specific DNAzyme: Insight into Function from Fluorescence Resonance Energy Transfer Studies. *Chem. Eur. J.* **17,** 13732–13742 (2011).
57. Organization, W. H. Uranium in drinking-water: Background document for development of WHO Guidelines for Drinking-water Quality. (2004).

Acknowledgements

This research was supported by the Public Welfare & Safety research program (NRF-2012M3A2A1051682, NRF-2012M3A2A1051686) through the National Research Foundation of Korea funded by the Ministry of Science, ICT and Future Planning (MSIP), Global Frontier Project (H-GUARD_2014M3A6B2060489) through the Center for BioNano Health-Guard funded by MSIP, and KRIBB initiative Research Program. H.K. is the

recipient of Global Ph.D. Fellowship (NRF-2011–0030947). Prof. Jong-Il Yun's RCLS (RadioChemistry and Laser Spectroscopy) lab at department of Nuclear & Quantum Engineering (KAIST, Daejeon) assisted the UO_2^{2+} and Th^{4+} related experiments.

Author Contributions

R.G. and H.K. conceived the main idea and executed the project equally. S.Y. and S.L. contributed to the treatment of biomaterials and related discussion. G. L., M. L. and C.R. contributed to the metal ions related discussion. T.K. and B.K. supervised the study. All authors also contributed to the manuscript preparations

Additional Information

Supplementary information accompanies this paper at http://www.nature.com/srep

Competing financial interests: The authors declare no competing financial interests.

How to cite this article: Gwak, R. *et al.* Precisely Determining Ultralow level UO_2^{2+} in Natural Water with Plasmonic Nanowire Interstice Sensor. *Sci. Rep.* **6**, 19646; doi: 10.1038/srep19646 (2016).